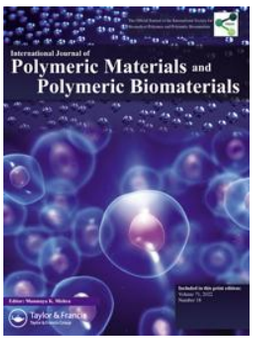

International Journal of Polymeric Materials and Polymeric Biomaterials

ISSN: (Print) (Online) Journal homepage: https://www.tandfonline.com/loi/gpom20

Preparation and characterization of self-stimuli conductive nerve regeneration conduit using co-electrospun nanofibers filled with gelatin-chitosan hydrogels containing polyaniline-graphene-ZnO nanoparticles

Hamideh Javidi, Ahmad Ramazani Saadatabadi, Seyed Khatiboleslam Sadrnezhaad & Najmeh Najmoddin

To cite this article: Hamideh Javidi, Ahmad Ramazani Saadatabadi, Seyed Khatiboleslam Sadrnezhaad & Najmeh Najmoddin (2022): Preparation and characterization of self-stimuli conductive nerve regeneration conduit using co-electrospun nanofibers filled with gelatin-chitosan hydrogels containing polyaniline-graphene-ZnO nanoparticles, International Journal of Polymeric Materials and Polymeric Biomaterials, DOI: 10.1080/00914037.2022.2133116

To link to this article: https://doi.org/10.1080/00914037.2022.2133116

Published online: 13 Oct 2022.

INTERNATIONAL JOURNAL OF POLYMERIC MATERIALS AND POLYMERIC BIOMATERIALS
https://doi.org/10.1080/00914037.2022.2133116

Preparation and characterization of self-stimuli conductive nerve regeneration conduit using co-electrospun nanofibers filled with gelatin-chitosan hydrogels containing polyaniline-graphene-ZnO nanoparticles

Hamideh Javidi[a], Ahmad Ramazani Saadatabadi[b], Seyed Khatiboleslam Sadrnezhaad[c], and Najmeh Najmoddin[a]

[a]Department of Biomedical Engineering, Science and Research Branch, Islamic Azad University, Tehran, Iran; [b]Chemical and Petroleum Engineering Department, Sharif University of Technology, Tehran, Iran; [c]Department of Materials Science and Engineering, Sharif University of Technology, Tehran, Iran

ABSTRACT

The core-shell structure conduit with conductive, antibacterial, and highly piezoelectric properties was designed and fabricated by a multi-step process. First, the shell structure was fabricated by rolling the co-electrospun mats of polycaprolactone/polyvinylidene fluoride and gelatin incorporated with polyaniline/graphene (PAG) nanocomposites. Then, the fabricated mats were filled with gelatin/chitosan hydrogels containing PAG and zinc oxide nanoparticles. Characterization of the intermediate materials and the final conduit revealed high electrical conductivity and remarkable output voltage for shell and core materials. MTT assay and antibacterial tests confirmed bioactivity and antibacterial properties of shells and cores. The results confirmed appropriateness of the conduit for nerve regeneration applications.

GRAPHICAL ABSTRACT

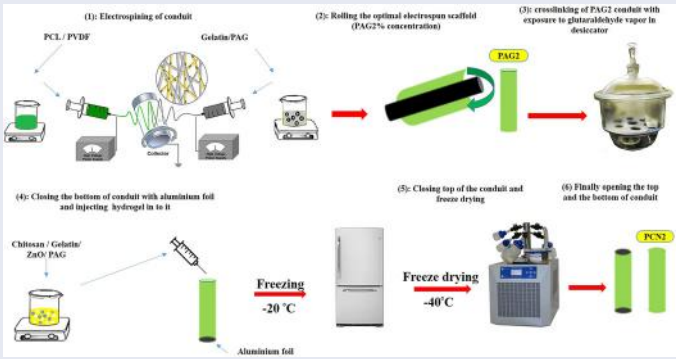

ARTICLE HISTORY
Received 25 August 2022
Accepted 3 October 2022

KEYWORD
Conductivity; Nerve guidance channels; Piezoelectricity; Polyaniline/graphene; PVDF

1. Introduction

Recently, interesting progresses have been made toward using tissue engineering as an alternative approach to conventional ones (i.e., autografts, xenografts and allografts) to repair and restore injured tissues[1]. Among various constructs developed for the regeneration of nerve tissues, artificial nerve guidance conduits (NGCs) with proper morphological and chemical properties can boost neural growth. In this regard, scaffold design and material selection are considered as two important factors for desirable nutrient and waste transport, mechanical stability, cellular interactions, and ultimately functional tissue formation[2,3].

Since nervous tissue contains a complex structure, it is crucial to design NGCs with superb features to suitably mimic the extracellular matrix (ECM)[1–3]. However, the lack of heterogeneity within most reported NGCs limits their performance to guide the development of new tissue. Therefore, the fabrication of NGCs with a special structure such as core-shell constructs containing gel/fibers structure is suggested[2,4]. It is expected that such engineered NGCs with high porosity in both core and shell similar to the ECM can promote cellular interaction[2]. Electrospinning is a versatile and cost-effective strategy for the fabrication of nanofibrous structures more closely matching the ECM architecture[1,5]. Furthermore, hydrogels can be ideal materials for tissue engineering due to their outstanding characteristics such as having a hydrated structure with high porosity[3,6].

For the fabrication of shell structure, polycaprolactone (PCL) was chosen due to its biocompatibility, biodegradabilityand

CONTACT Ahmad Ramazani Saadatabadi ramazani@sharif.edu Chemical and Petroleum Engineering Department, Sharif University of Technology, Tehran, Iran; Najmeh Najmoddin najmoddin@srbiau.ac.ir Department of Biomedical Engineering, Science and Research Branch, Islamic Azad University, Tehran, Iran.

providing integrity and mechanical properties of the shell[1,5,7,8]. However, its hydrophobicity and poor biological properties could be compensated using natural polymer such as gelatin (GEL). Therefore, gelatin was co-electrospun with PCL to improve cell attachment and proliferation[1,5,7,9,10]. Since gelatin suffers from poor mechanical strength and a high degradation rate, cross-linking agents such as glutaraldehyde and genipin can be used to overcome such drawbacks[5,11]. Chitosan (Cs), derived from deacetylation of chitin is a biocompatible polymer that could accelerate tissue regeneration[12,13]. However, the bioactivity of CS is weak and hence biologically active materials like gelatin are blended[8,13,14]. The combination of Cs and gelatin was used to prepare hydrogel structure as a core section of NGCs[6,15].

Many research endeavors suggested that electrical stimuli play a crucial role in controlling cell function such as proliferation, differentiation and migration of nerve cells[1,16–18]. Provision of electrical stimuli requires invasive transcutaneous devices or percutaneous electrodes which is inconvenient for the patients[19]. Utilization of piezoelectric materials (i.e., Polyvinylidene fluoride (PVDF), zinc oxide (ZnO)) with the ability of inducing localized electrical stimulation within the body in a wireless fashion could be a good solution to this problem. Piezoelectric micro/nano fibers are found in applications in the biomedical field due to their high sensitivity to mild mechanical stress/strain. PVDF as a well-known piezoelectric organic platform is biocompatible, lightweight, flexible and electroactive, while ZnO is a piezoelectric ceramics and exhibits high piezoelectric constant[19–25]. Try has been made to improve the performance of PVDF by inclusion of appropriate stimulus agents (i.e., nanomaterials). Polyaniline/graphene (PAG) with excellent chemical stability and highly electric conductivity has been applied in the fabrication of tissue-engineered scaffolds[2,16–18]. Soleimani et al. showed nanoparticles of PAG nanocomposite could enhance cell growth on a PCL/gelatin-based scaffold[18]. Mohammadi et al. observed significant enhancement in electrical conductivity of chitosan/gelatin-based electrospun multichannel using PAG nanoparticles for neural growth[5]. Bayat et al. showed the improvement of conductivity for cell stimulation and growth by exploiting PAG nanoparticles for alginate/PAG conduit[16]. Mohseni et al. reported cell growth in the conductive self-electrical stimuli bioactive scaffold using chopped electrospun piezoelectric nanofibers of PVDF/mesoporous silica nanoparticle incorporated in gellan/PAG) nanocomposites[17]. Abzan et al. shown non-solvent induced phase separation method to develop PVDF/graphene oxide (GO) scaffold for nerve tissue engineering and resulted that the incorporation of GO sheets to PVDF scaffold could increase the piezoelectric property[26]. Moreover, ZnO nanoparticles are well-known antibacterial agents which could prevent the growth of microorganisms through different mechanisms such as the formation of reactive oxygen species, release of Zn^{2+} ions, etc. resulting in destructing bacterial cell integrity[27]. The incorporation of ZnO nanoparticles donates antibacterial activity to the NGCs which could prevent initial inflammation during the scaffold placement in the body.

Although many studies have been conducted to design and fabricate NGCs with the most favorite properties for cell growth and nerve regeneration, to the best of our knowledge, structural conductive conduits with core-shell structure with self-stimuli and antibacterial properties have not been reported. So, in this study, a novel structural nerve regeneration channel consisting of co-electrospun membrane and freeze-dried hydrogel was developed to act as shell and core materials, respectively. PVDF was used as a piezoelectric material in the shell structure, while ZnO was added to gelatin to increase piezoelectric properties as well as to adjust antibacterial and the degradation rate of the conduits. Meanwhile, PAG nanoparticles were used to promote the electrical conductivity and help to increase output voltage of NGCs. Finally, the physical, chemical, and biological properties of fabricated NGCs were evaluated.

2. Materials and methods

2.1. Materials

PCL pellets (M_n = 80,000 g. mol^{-1}), Polyvinylidene fluoride (PVDF; M_n = 270,000 g. mol^{-1}), aniline monomer was obtained from Sigma–Aldrich, and prior to use the aniline monomer was purified by vacuum distillation and was stored at 4 °C, gelatin (porcine skin type A powder), chitosan (Cs; deacetylation 75–85%), ammonium peroxydisulfate (APS), sodium dodecyl sulfate (SDS), graphene, MTT (3(4, −5-dimethylthiazol-2-yl)-2,5-diphenyltetrazolium bromide), phosphate-buffered saline (PBS), fetal bovine serum (FBS), penicillin-streptomycin, and trypsin- ethylenediaminetetraacetic acid (EDTA), dey-engley neutralizing broth (DE), were all purchased from Sigma-Aldrich. The hydrochloric acid (HCl), glacial acetic acid, N, N-dimethylformamide (DMF), ethanol, methanol, trypton soy agar (TSA), and acetone were obtained from Merck (Germany). Glutaraldehyde solution (GTA; 50%) was supplied by Beijing Chemical Reagents. Dulbecco's Modified Eagle Medium/Nutrient Mixture F-12 (DMEM/F12) was obtained from Gibco Invitrogen. ZnO with a purity of over 99.5% was made by Bonyan Shimi Company.

2.2. Synthesis of polyaniline/graphene nanoparticles

The synthesis of polyaniline/graphene (PAG) was based on the method reported in Ref.[17]. First, 5 g graphene was ultrasonically dispersed in 100 mL HCl (1 M) containing aniline monomer. Next, 5.767 g SDS was added to the mixture at room temperature under the nitrogen atmosphere. Then, 0.913 g APS was poured slowly within 20–30 min. The polymerization was carried out under a magnetic stirrer for 6 h which resulted in altering the color of the solution from milky to blue. After completion of the reaction by keeping the mixture at room temperature for a further 24 h, methanol was added. To remove unreacted agents, the obtained product was washed with ethanol, methanol, and distilled

water several times and finally PAG nanocomposite was dried in an oven at 50 °C for 48 h.

2.3. Fabrication of electrospun scaffold for shell structure

PCL (13% w/v in acetone) and PVDF (19% w/v in DMF) solutions were prepared by dissolving the polymers at 37 °C for 4 h and preserved under magnetic stirring for 12 h at room temperature. The PCL-PVDF solution was obtained by mixing the mentioned solutions (acetone to DMF ratio ~ 50:50). A solution of 32% w/v of gelatin was also prepared in acetic acid: water (60:40). The PAG nanocomposite was dispersed in distilled water homogeneously using ultrasonication and then was added to the gelatin solution at different percentages (0, 1, 2, 3 wt. %). 5 mL of each solution was loaded on the syringe and both of them co-electrospun for 6 h using 22—a gauge needle. The electrospinning parameters were set for each solution as follows: (I) syringe containing PCL/PVDF solution, flow rate: 0.5 mL/h, tip-collector distance: 15 cm, applied voltage: 13 kV, the rotating speed: 350 rpm; and (II) syringe containing gelatin/PAG nanocomposite, flow rate: 0.2 mL/h, tip-collector distance: 16 cm, applied voltage: 10 kV and the rotating speed: 350 rpm. The prepared scaffolds were then dried in a vacuum oven for 20 h.

2.4. Preparation of chitosan–gelatin hydrogel to be used for core structure

First, 1% w/v solution of chitosan and gelatin was separately prepared in acetic acid and distilled water, respectively. Then both solutions were mixed under magnetic stirring for 30 min. After that, dispersed PAG nanoparticles (2% w/v) and ZnO nanoparticles (1% w/v) in distilled water were added separately to the chitosan-gelatin solution one after another.

2.5. Preparation of structural conduit

Rectangular pieces of electrospun nanocomposite scaffolds with 0, 1, 2, 3 wt% of PAG nanoparticles were rolled around a Teflon tube and formed into a channel. The rolled form of fibers was placed in the chamber of GTA steam (2.5% v/v) for 48 h. The obtained scaffolds were nominated as PAG0, PAG1, PAG2, PAG3 according to the PAG concentrations. For the fabrication of conduit with core/shell structure, one side of the channel was covered with aluminum foil and the prepared hydrogel was injected from the other side. Finally, the other side of the channel was also covered with aluminum foil, and placed in the freeze-drier. This sample was nominated as PCN2. For comparison reason, one conduit was also filled with hydrogel without any PAG and nominated as PCN0.

3. Characterization

3.1. Characterization of PAG nanocomposite

Morphological properties of PAG nanocomposite were studied via scanning electron microscopy (SEM, TESCAN: Mria3, Czech Republic), and Dynamic Light Scattering (DLS, Nano-ZS; Malvern, UK). The chemical structure of polyaniline-graphene was assessed by Fourier-transform infrared spectroscopy (FTIR, Bruker, Ettlingen, Germany) in the range of 4,000–400 cm^{-1} using the KBr pellets technique.

3.2. Scaffold characterization

The electrospun scaffolds were examined via SEM (TESCAN: Mria3, Czech Republic) at 25 kV for textural evaluation. The functional groups were assessed by FTIR (Bruker, Ettlingen, Germany) in the range of 4,000–500 cm^{-1}. The wettability of the electrospun scaffold was evaluated using a contact angle meter (DSA25E, Kruss GmbH, Germany).

3.3. Hydrogel analysis

Surface characterization of hydrogels was carried out by SEM (TESCAN: Mria3, Czech Republic).

To assess the water uptake capacity of the hydrogels, each sample was immersed into PBS at 37 °C. At each time point (30 min, 1 h, 3 h, 4 h, 24 h, 48 h, 72 h), the samples were removed and excess water was eliminated by a filter paper. Then, the water uptake (Q_m) was calculated through Eq. 1:

$$Q_m(\%) = \frac{W_s - W_d}{W_d} \times 100\% \quad (1)$$

Where W_d and W_s were the weights of dry and wet samples, respectively.

To measure the rate of *in vitro* degradation, the samples were placed in a 24-well plate and each well was filled with PBS. Then, the samples were placed in an incubator at 37 °C with 60 rpm rotation for 3, 7 and 14 days. The *in vitro* degradation was calculated by Eq. 2:

$$D(\%) = \frac{W_d - W_f}{W_d} \times 100\% \quad (2)$$

Where W_d and W_f were the weight of hydrogels before and after soaking into PBS, respectively.

The antibacterial activity of the fabricated hydrogel was evaluated by half-McFarland standard method using colony count unit (CFU), against both *Staphylococcus aureus PTCC1112* (*S. aureus*) and *Escherichia coli PTCC1399* (*E. coli*) as a Gram-positive and Gram-negative bacteria, respectively. In this regard, a half-McFarland suspension was prepared from bacteria strain. Chitosan–gelatin hydrogel containing 1% ZnO nanoparticle was prepared in 10 × 10 mm size and were placed in an agar liquid and allowed to dry the gel. Then, the sample was cut with dried

gel. After sterilization, the sample was incubated at 37° C for 24 h. At the appropriate contact time, DE neutralizer was added to each sample at a dilution of 1:10 and the sample was sonicated for 1 min. Then, the suspension was cultured in TSA medium and the plates were incubated for 34 h. Finally, the number of viable bacterial colonies was counted. To evaluate the anti-bacterial activity, the following equation was used.

$$\text{Antibacterial efficiency}\,(\%) = \frac{\text{CFUcontrol} - \text{CFUsample}}{\text{CFUcontrol}} \times 100\%, \tag{3}$$

where $CFU_{control}$ and CFU_{sample} are the average number of bacteria in the control and the chitosan–gelatin hydrogel containing 1% ZnO nanoparticles, respectively.

3.4. Conduit characterization

3.4.1. Piezoelectric and conductivity measurements

To investigate the piezoelectric property, a movable arm that can produce mechanical force was utilized. Two aluminum foil was attached to the samples, and the electrical conductivity was measured by an oscilloscope.

The four-point probe method was used to calculate the electrical conductivity, where the rate of current (I) was 0.6 mA in Eq. 3:

$$\sigma = Ln2/\pi\ t\ (I/V), \tag{4}$$

where σ, I, V, and t were electrical conductivity (S/cm), current (A), voltage (V), and sample thickness (cm), respectively[28].

3.4.2. Degradation test

The rate of *in vitro* degradation of fabricated conduits was calculated as mentioned in Section 3.3.

3.5. Assessment of cell viability and proliferation

The cell viability and proliferation of PC12 cultured on the fabricated conduit were assessed by the 3-[4, 5-dimethylthiazoyl-2-yl] 2,5-diphenyl tetrazolium bromide (MTT) assay after 1 and 3 days.

First, the PC12 cells were seeded in DMEM/F12 containing 10% FBSand 1% antibiotic (penicillin-streptomycin) for 24 h. To perform the MTT assay, the prepared conduits were sterilized in alcohol (70% v/v). Then, the PC12 cells were cultured at the density of 1×10^4 cells on each conduit, considering cells seeded on Tissue Culture Polystyrene (TCPS) as a control. Samples were incubated at 37 °C and 5% CO_2. To assess the cell viability at 1 and 3 days, 100 µL MTT solution (0.3 mg/mL in PBS) was added to each well and incubated for 3 h. Finally, the medium was removed and replaced with dimethyl sulfoxide (DMSO, 100 µL), and the cell viability at the wavelength of 570 nm through ELISA reader was recorded. The cell viability (%) was assessed by Eq. 4:

$$\text{Cell viability}\ (\%) = \frac{OD_{sample}}{OD_{control}} \times 100\%. \tag{5}$$

The results were reported based on mean ± SD, $n = 3$.

3.6. Statistical analysis

The data were expressed based on mean ± SD. GraphPad, Prism software (V.9, USA) was used to perform one-way ANOVA for statistical of results. The probability values less than 0.05 (p-value <0.05) were considered significant.

4. Results

4.1. PAG nanocomposite

The morphological characteristic of PAG nanocomposite was observed via SEM images. Figure 1a shows that the particles have a spherical shape with an average size of 254 ± 36 nm. In addition, the average size of particles from the DLS technique was found to be 330 ± 91 nm.

The FTIR spectrum of the synthesized PAG nanocomposite is shown in Figure 1b. The characteristic peak at 3,400 cm^{-1} is corresponded to N–H stretching, as well as the peaks in the range of 1,500–1,600 cm^{-1} is attributed to the stretching of C–N of the benzenes and quinonics. Moreover, the peaks at 540 cm^{-1} and 1,100 cm^{-1} were assigned to the SO^{3-} group from SDS and the delocalization of electrical charges, respectively, confirming the successful formation of PAG nanocomposite[17].

4.2. Characterization of nanofibrous scaffold

In this study, the design and fabrication of conductive nerve guidance channels with core-shell structure were performed. First, the NGCs with the fibrous structure were fabricated through co-electrospinning of PCL/PVDF and PAG nanocomposite incorporated gelatin. SEM micrographs of fibrous scaffolds containing various amounts of PAG nanocomposite are shown in Figure 2a–d. Fibers were prepared smooth and uniform in structure without any beads in all samples. The mean fiber diameter of PAG0, PAG1, PAG2, and PAG3 was 461 ± 122, 324 ± 99, 236 ± 85, 243 ± 143, respectively. The fiber diameter decreased with the increment of PAG nanocomposite content which may be due to the enhancement of electrical conductivity. The presence of PAG nanocomposite in fibers also could have a positive effect on the preparation of smooth electrospun fibers. It is noteworthy that the presence of PVDF has been effective in decreasing the viscosity of the solution[17].

To assess the functional groups of scaffolds containing different percentages of PAG nanocomposite (PAG0, PAG1, PAG2, PAG3), FTIR analysis was carried out and the result is shown in Figure 3. The peak at 3,400 cm^{-1} was related to N–H stretching. In addition, the bands in the range of 1,500–1,600 cm^{-1} belonged to the stretching of C–N of the benzenes and quinonics which confirmed the presence of PAG nanocomposite in the fabricated fibers[28]. The bands

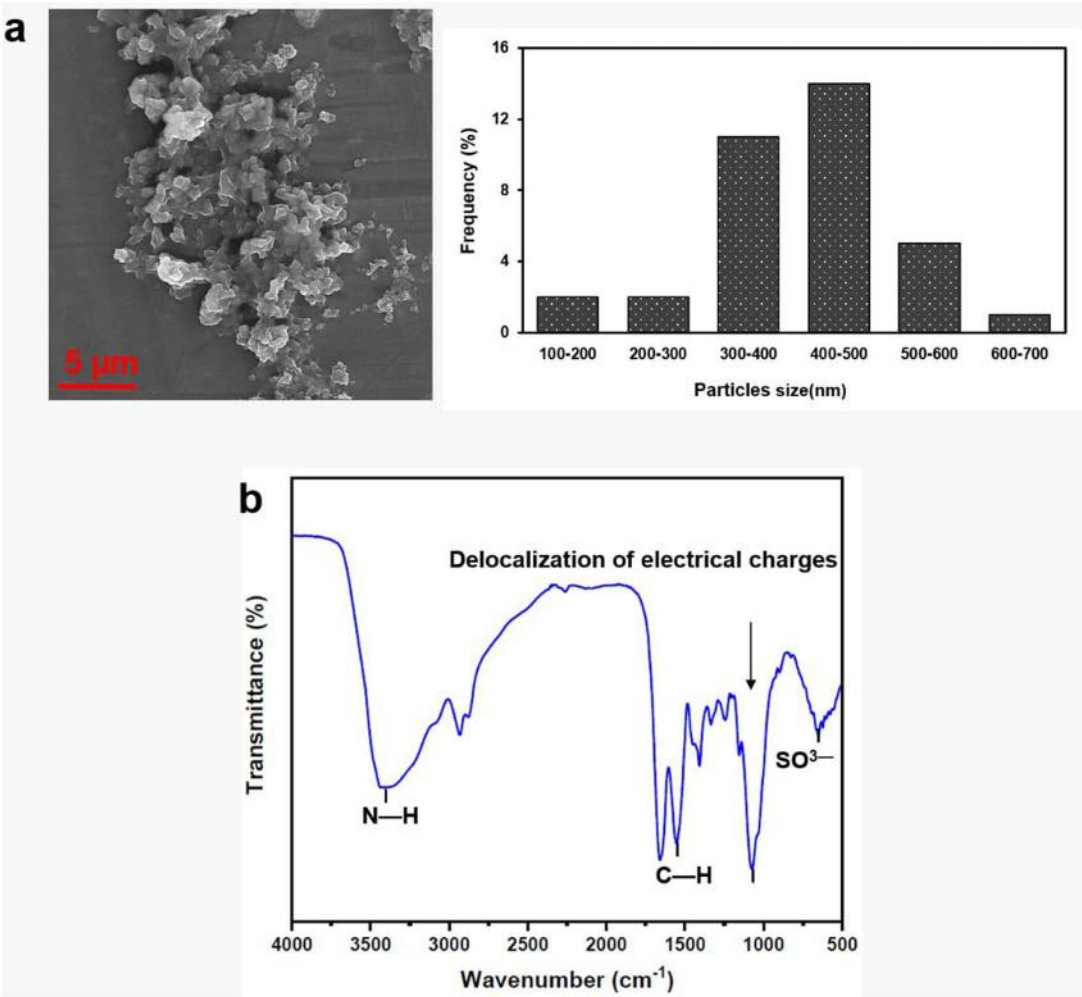

Figure 1. SEM image of synthesized PAG nanocomposite and average particle size of PAG nanocomposite obtained by image analyzing method (a), AT-FTIR spectrum of polyaniline-graphene nanocomposite (b).

related to the β-PVDF also were detected at 879 cm^{-1} and 1,237 cm^{-1}[29,30]. The peaks of PCL were characterized as follows: 2,932 cm^{-1} (asymmetric CH_2 stretching), 1,724 cm^{-1} (carbonyl C=O stretching), 1,296 cm^{-1} (C–O and C–C stretching), 1,240 cm^{-1} (asymmetric C–O–C stretching). The bands of gelatin were recognizable through Figure 3, where the bands at 3,400 cm^{-1}, 1,645 cm^{-1}, 1,540 cm^{-1}, and 1,240 cm^{-1} were ascribed to the N–H stretching, C=O vibrations, C–N stretching and N–H, respectively[5,13].

The contact angle assessment, known as one of the most important factors in the interaction of scaffold/cells, was performed and the results are shown in Figure 4[5]. PCL and PVDF are hydrophobic polymers in nature[5,31,32]. However, the presence of gelatin improves hydrophilicity[5]. As can be seen, incorporation of PAG nanocomposite into the scaffolds enhances the wettability up to 55° ± 1° (2% PAG), while increasing PAG nanocomposite up to 3% w/v resulted in decreasing hydrophilicity.

4.3. Characterization of hydrogel

SEM image of CS/gelatin hydrogel containing PAG and ZnO is shown in Figure 5. The average size of ZnO nanoparticles was 252 ± 39 nm (Figure 5a), and the average cavity size was around 221 ± 106 nm (Figure 5b).

In vitro degradation assay shows a significant difference between the degradation rate of hydrogel in the absence and presence of 2% PAG after 14 days (Figure 6a). The water uptake test reveals that the swelling ratio of both hydrogels without and with 2% PAG decreases after 72 h (Figure 6b).

The antibacterial test results for CS/GEL hydrogel containing 1% ZnO nanoparticles obtaining according to CFU method against both S. aureus and *E. coli* bacteria strain are presented in Figure 6c. Obtained data indicated that the hydrogel present 46% and 45% inhibition growth on S. aureus and *E. coli* bacteria strain and has good potential antibactericidal properties for biomedical applications.

4.4. Characterization of shell conduit

The piezoelectric property and electrical conductivity of the prepared conduits are presented in Figure 7 and Table 1, respectively.

The output voltages obtained from piezoelectric tests for PAG0, PAG1, PAG2, and PAG3 are 300 ± 0.4, 700 ± 0.2, 900 ± 0.3, and 800 ± 0.2 mV, respectively (Figure 7). The results show that incorporation of PAG nanocomposite up

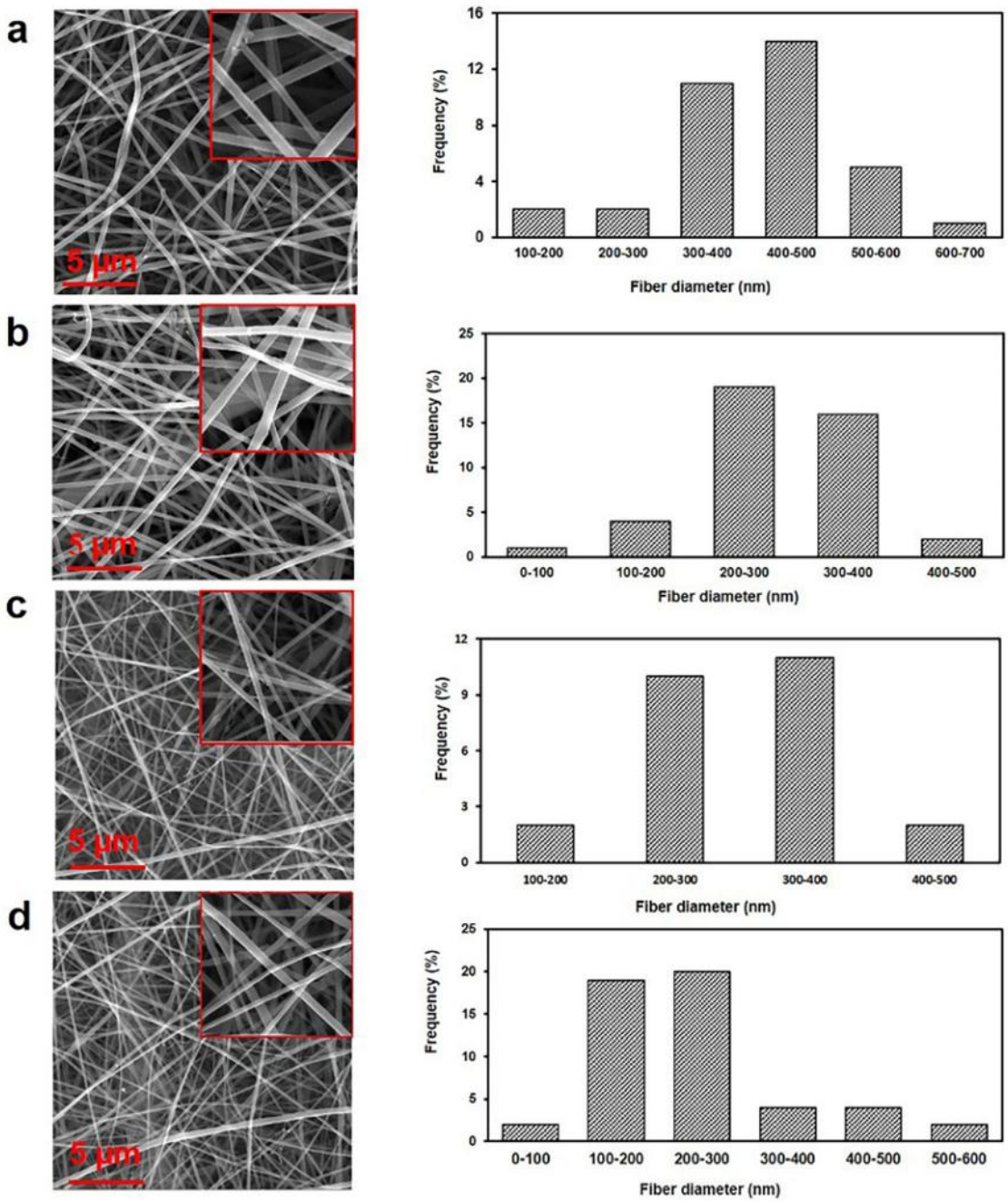

Figure 2. FESEM micrographs and mean fibers diameter of PAG0 (a), PAG1 (b), PAG2 (c), and PAG3 (d).

to 2% enhances the output voltage of the conduit, while higher amount of PAG nanocomposite decreases the output voltage during conduit mechanical deformation. Moreover, the conduit with core-shell structure which was filled with hydrogel in the core section reveals a higher amount of output voltage up to 940 ± 0.5 mV for PCN0 (without PAG2 in the core) and 1,000 ± 0.2 mV for PCN2 (with PAG2 in the core) in Figure 7. ZnO and PAG have a synergic effect, which increases the output voltage, confirming the enhancement of piezoelectric property. The same behavior also could be observed in Table 1 for the conductivity of fabricated conduits.

The rate of degradation is a vital factor affecting the conduit stability in the biological environment. PCL and PVDF suffer from low hydrophilicity which represents low *in vitro* degradation[5,31,32]. Moreover, the degradation ratio shows a descending trend with increasing PAG nanocomposite concentrations[5]. However, PCN2 shows higher *in vitro* degradation which may be attributed to the higher hydrophilicity of Cs-gelatin hydrogels in the core section of the conduit[6,8] (Figure 8a). It is worth mentioning that the presence of 1% ZnO may have a positive role on the degradation rate and swelling ratio of the conduit[13].

The MTT assay was performed to evaluate the cell viability and proliferation of fibrous scaffold with 2% PAG as well as a conduit with core-shell structure after 1 and 3 days (Figure 8b). As can be seen, there is a significant difference between both samples and the control group (p value <

0.05). Moreover, cell viability is higher for PCN2 with fiber-gel structure than PAG2 with only fibrous structure. This could be attributed to the hydrophilic nature of Cs-gelatin hydrogel resulting in improvement in cell proliferation[33,34]. It has been reported that the agglomeration of ZnO nanoparticles in the polymer matrix can increase the size of nanoparticles and causes toxicity. The desirable viability of PCN2 containing 1% ZnO could be a sign of good distribution of ZnO nanoparticles in the hydrogel[35,36].

5. Discussion

The peripheral nerve system has some limitations in reconstructing axonal defects with larger than 5 mm gaps. Using allografts and autografts to solve this problem has several disadvantages such as donor site morbidity, limitation in nerve supply and loss of functionality. Nerve guidance channel, known as conduit has been considered as an ideal alternative that can improve the rate of nerve tissue regeneration through simulating the targeted tissue microenvironment. An ideal conduit possesses some characteristics, including non-carcinogenicity and non-toxicity, simulating axonal growth, biodegradability through natural systemic absorption tailored with axonal regeneration, and providing good mechanical and physical properties in the duration of surgeries and further studies[37]. Since there is a strong relation between the structural features and composition of fabricated conduit and its interaction with the biological system, it is necessary to design an engineered construct to fulfill mentioned characteristics. According to the reports, many synthetic and natural polymers have been used to fabricate conduit channels[37]. However, natural polymers, including gelatin present a lack of mechanical strength which can limit the functionality of the prepared conduit[5,7]. On the other hand, synthetic polymers such as PCL suffer from a lack of hydrophilicity, and the biological properties of synthetic polymers are poor[5,7]. Therefore, the production of scaffolds using a co-electrospinning technique from both natural and synthetic polymers would be beneficial in this regard[1]. Moreover, rolling the fibrous mat and filling it with hydrophilic hydrogels such as chitosan/gelatin would have a positive effect on the biological properties of the conduit[1,5]. The presence of piezoelectric materials such as PVDF and ZnO probably led to the generation of localized charges[20,38]. Interestingly, studies have indicated an aligned relationship between electrical conductivity and nerve reconstruction, and conductive materials can help a higher rate of regeneration[10]. PAG nanocomposite has taken considerable attention to improve electrical and mechanical properties as well as the wettability of the conduit[1,5,39]. So, design and fabrication of a structural conductive nerve guidance conduit using PCL-PVDF-gelatin co-electrospun fibers filled with a gelatin-chitosan hydrogel containing polyaniline-graphene-ZnO nanoparticles has been performed in this work.

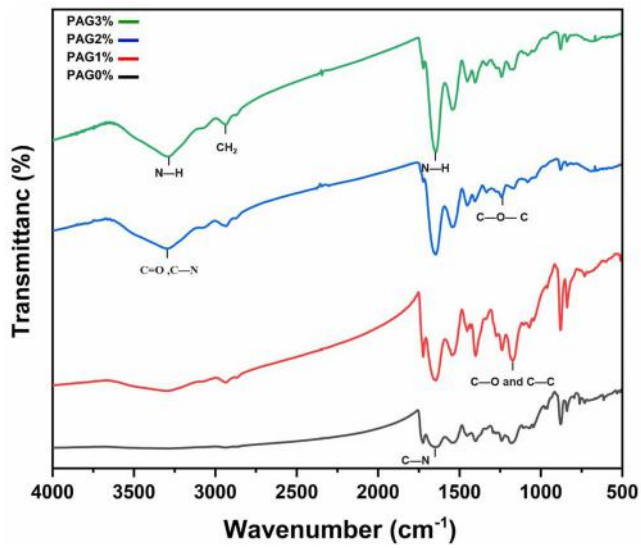

Figure 3. FTIR spectra of PAG0, PAG1, PAG2, and PAG3 fibrous mats (shell of conduit).

The results of SEM micrographs and characterization of functional groups showed that PAG nanocomposite was successfully incorporated into PCL-PVDF-gelatin fibers. The water contact angle assessment indicated the enhancement of the wettability of conduit shell by increasing PAG nanocomposite content up to 2 wt.% which could be due to change of surface roughness of electrospun mat. Incorporation of a higher amount of PAG nanocomposite resulted in decreasing the hydrophilicity, which could be related to the aggregation/agglomeration effect of PAG nanocomposite[36]. It is worthwhile to mention that the incorporation of PAG in the hydrogel did not significantly alter the water uptake, which is recognized as an important characteristic of the scaffold affecting the cellular interactions. The degradation rate of NGCs is one of the main

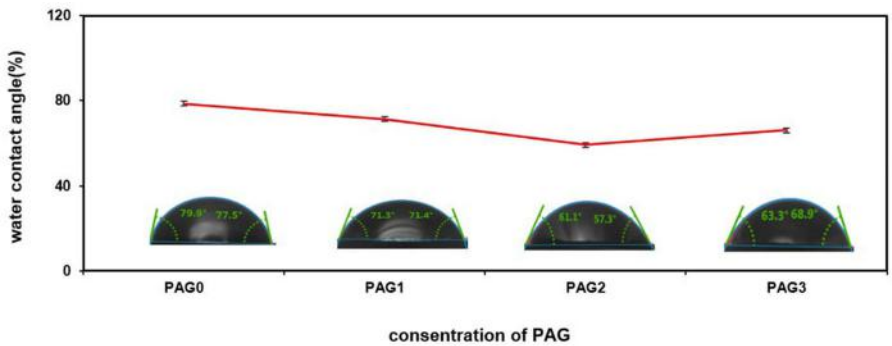

Figure 4. The average contact angle of PAG0, PAG1, PAG2, and PAG3 fibrous mats.

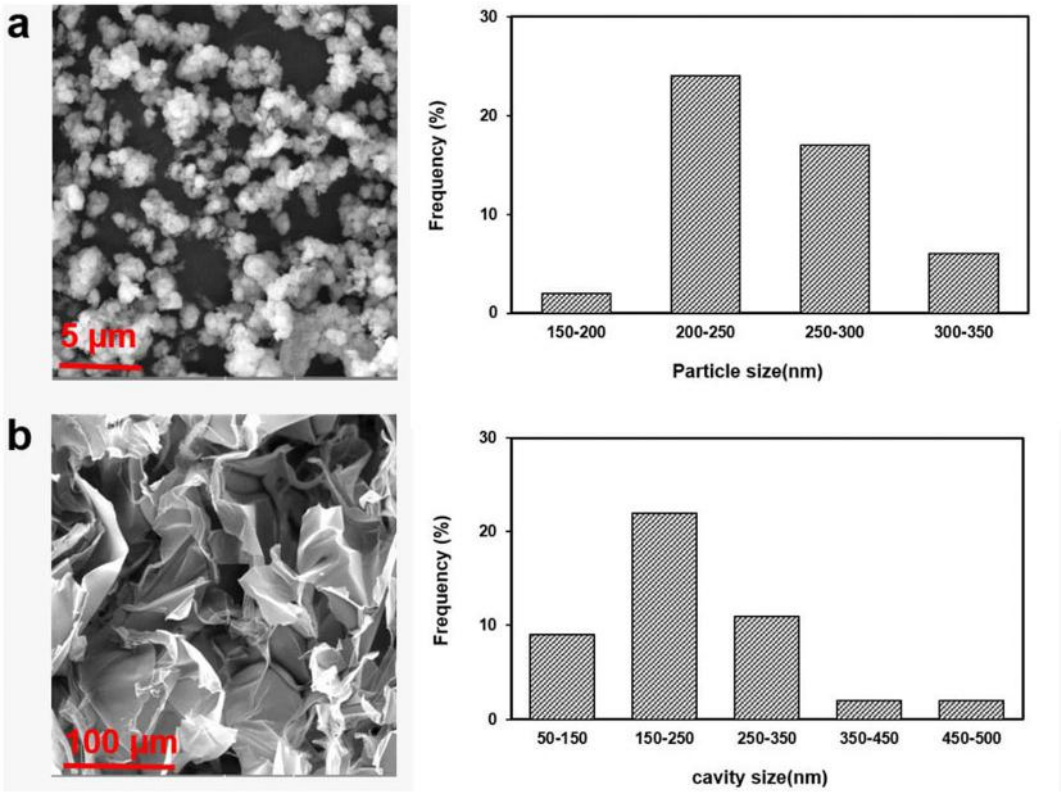

Figure 5. FESEM micrographs of ZnO nanoparticles with a purity of 99.5%, and particles diameter size of ZnO nanoparticles (a) and the CS–GEL/ZnO (1%)/PAG (2%) hydrogel and distribution chart of cavity size of hydrogel (b).

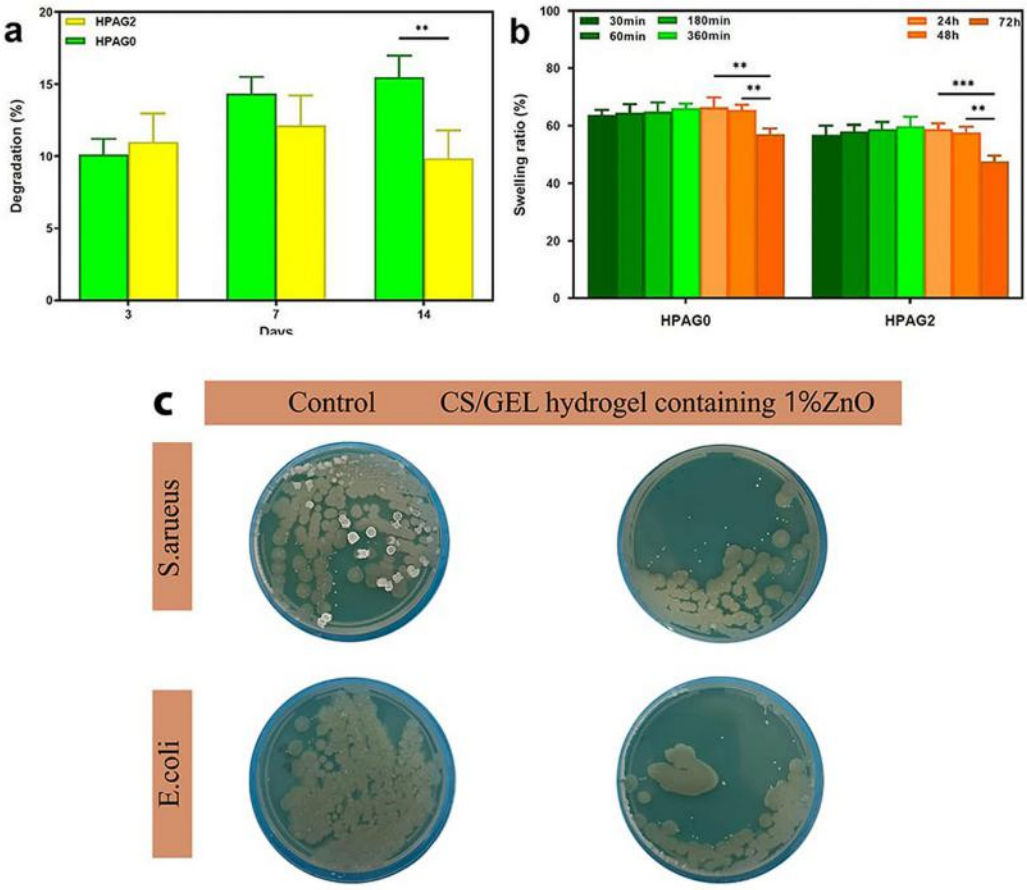

Figure 6. Degradation rate of (CS–GEL/ZnO (1%)/PAG (0%)) hydrogel (HPAG0), and (CS–GEL/ZnO (1%)/PAG (2%)) hydrogel (HPGA2) (a) and Swelling ratio of (HPAG0, HPAG2) (b). Values are mean ± SD ($n = 3$). *Significantly different from conduits, **$p < 0.005$; Antibacterial activity of CS–GEL hydrogel with and without 1% ZnO (c).

factors affecting the nerve regeneration process. It is expected that the degradation rate of biomaterial has consistency with the regeneration rate of new nerve tissue. So, during the degradation process the stability of NGC should be preserved. As shown in Figures 6 and 8, increasing the PAG nanocomposite decreases the degradation rate of both shell and core sections of conduit. The obtained results were fully consistent with the work reported elsewhere by Mohammadi et al. They have also reported that incorporation of crystalline PAG nanocomposite into the scaffolds leads to the reduction of degradation rate. However, filling the conduit with hydrogel enhances the degradation rate of the whole construct thanks to the presence of amorphous hydrophilic gelatin with a high degradation rate. Moreover, the presence of 1% ZnO may also have contributed to the increment of the degradation rate and swelling ratio of the conduit[13].

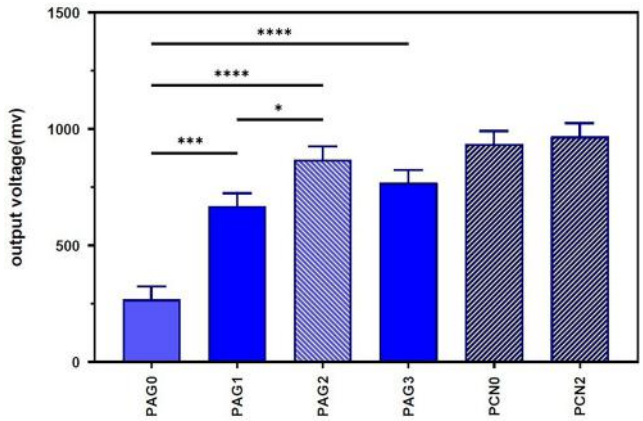

Figure 7. Effects of PAG nanocomposite concentration (PAG0, PAG1, PAG2, and PAG3) and filling hydrogel (PCN2, PCN0) on the output voltages of the self-stimuli prepared conduits. Values are mean ± SD ($n = 3$). *Significantly different from conduits, *$p < 0.05$, ***$p < 0.0005$, ****$p < 0.0001$.

Table. 1. Electrical conductivity of the prepared conduits with different percentages of PAG nanoparticles, and the one filled with hydrogel (PCN2).

Samples	PAG0	PAG1	PAG2	PAG3	PCN2
Conductivity (s/cm)	0	5.5×10^{-5}	7.6×10^{-5}	6.7×10^{-5}	8.9×10^{-5}

Many researchers stated that conductive cue is a key element for nerve signal conduction and thereby improving nerve regeneration. Song et al. reported that fibrous conduit with the electrical property of 2.4×10^{-5} S/cm was favorable for electrical stimulation of nerve cells to repair 15 mm gap sciatic nerves in rats (Table 1)[40]. Using piezoelectric materials with the capability of producing an electrical signal in condition of conduit deformation could be effective way to produce insitue electrical signal. Here, the piezoelectric and electrical conductivity of prepared conduit with and without hydrogel was evaluated. As shown in Figure 6, the ascending trend of recorded voltage up to 900 ± 0.3 mV by loading 2% of PAG nanocomposite was detected. Increasing the PAG nanocomposite to 3% causes the decrement of the output voltage to 800 ± 0.2 mV (Figure 7), which could be attributed to the agglomeration of particles in the membrane. Moreover, filling the conduit by hydrogel containing PAG and ZnO resulted in increment of output voltage up to 940 ± 0.5 mV for PCN0 and 1,000 ± 0.2 mV for PCN2 (Figure 7). β phase increase piezoelectric properties in PVDF, and nucleating particles such as ZnO and graphene could have synergistic effect on piezoelectric properties of PVDF[41,42]. Therefore, the presence of 2% PAG nanocomposite as well as 1% ZnO in PCN2 has significant piezoelectric property. A similar trend was also observed for the electrical conductivity of the conduit measured via a four-point probe device. As shown in Table 1, the conductivity of conduits has a direct relationship with PAG content. The addition of PAG to the conduit increases the conductivity from virtually an insulator's conductivity for PAG0 conduit to 7.6×10^{-5} S/cm for PAG2 conduit and 8.9×10^{-5} S/cm for PCN2 (Table 1). PAG was utilized as a conductive substrate to have a positive effect on both electric and piezoelectric properties of the final core-shell conduit. The developed conduit in this research with electrical and piezoelectric features could provide a suitable environment for the axonal outgrowth. The results of the MTT assay demonstrated that PC12 cells were proliferated on PAG2 and PCN2 conduit better than the control sample (p value < 0.05). Moreover, filling the conduit with hydrogels containing PAG and ZnO boosted the viability and proliferation of

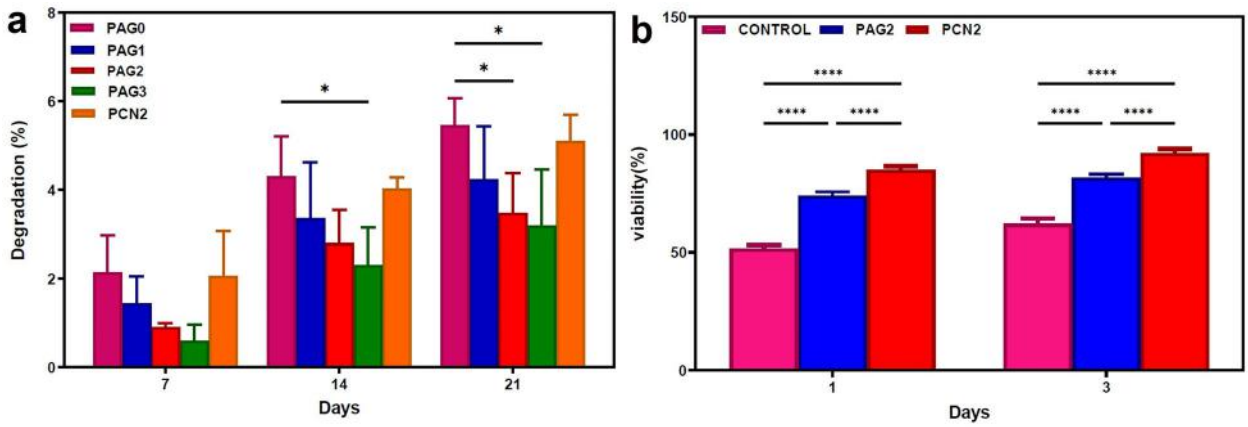

Figure 8. The rate of *in vitro* degradation of electrospinning scaffolds containing different percentages of PAG nanoparticles (PAG0, PAG1, PAG2, and PAG3), and the conduit filled with hydrogel (PCN2) (a). MTT assay of fibrous mat with 2% PAG (PAG2), and the conduit filled with hydrogel (PCN2) (b). Values are mean ± SD ($n = 3$). *Significantly different from conduits, *$p < 0.05$, **$p < 0.005$, ***$p < 0.0005$, ****$p < 0.0001$.

PC12 cells, which could be attributed to the natural feature of hydrogels.

6. Conclusions

In intense disorders, spontaneous nerve regeneration/reconstruction cannot happen, and even after medical surgeries, the injured nerve would not fully be rehabilitated. In this case, using a nerve regeneration guidance channel can be a helpful therapy that allows axonal growth from the proximal to the distal stump. In the present study, a novel conduit consisting of a self-stimuli electrospun shell and a hydrogel core with both electrical and piezoelectric properties was developed. Mats of PCL/PVDF electrospun fibers and gelatin containing polyaniline-graphene (PAG) nanocomposite fibers were produced by co-electrospinning technique. Contact angle measurement showed that the hydrophilicity of the shell was increased by addition of 2% of PAG nanoparticles. Then, the electrospun mat was formed into a tube by rolling process and curing it at appropriate condition. Finally, the prepared tube was filled with hydrogels consisting of gelatin/chitosan loaded with PAG and ZnO nanoparticles. The produced conduit showed significant piezoelectric properties and output voltage was enhanced up to approximately 1,000 mV with introduction of ZnO nanoparticles in the injected gelatin into the conduit. MTT assessment showed that filling the electrospun conduit with a hydrophilic hydrogel containing PAG and ZnO promoted PC12 cell growth, significantly. The fiber-gel conduit with core-shell structure containing piezo and conductive species could serve as an effective scaffold for nerve regeneration process. Our future studies will investigate the potential of such conduit on the neural differentiation of PC12 cell and in vivo animal nerve regeneration experiments.

CRediT authorship contribution statement

Hamideh Javidi: Methodology, Investigation, Resources and Software, Writing-Original draft. Ahmad Ramazani: Supervision, Conceptualization, Reviewing and Editing. Seyed Khatiboleslam Sadrnezhaad: Supervision, Reviewing and Editing. Najmeh Najmoddin: Interpretation of data, Reviewing and Editing.

Disclosure statement

The authors declare no potential conflicts of interest with respect to the research, authorship, and/or publication of this article.

References

[1] Heidari, M.; Bahrami, S. H.; Ranjbar-Mohammadi, M.; Milan, P. B. Smart Electrospun Nanofibers Containing PCL/Gelatin/Graphene Oxide for Application in Nerve Tissue Engineering. *Mater. Sci. Eng. C Mater. Biol. Appl.* **2019**, *103*, 109768. DOI: 10.1016/j.msec.2019.109768.

[2] Sarker, M.; Naghieh, S.; McInnes, A. D.; Schreyer, D. J.; Chen, X. Strategic Design and Fabrication of Nerve Guidance Conduits for Peripheral Nerve Regeneration. *Biotechnol. J.* **2018**, *13*, e1700635. DOI: 10.1002/biot.201700635.

[3] Wang, Y.; Tan, H.; Hui, X. Biomaterial Scaffolds in Regenerative Therapy of the Central Nervous System. *Biomed. Res. Int.* **2018**, *2018*, 7848901. DOI: 10.1155/2018/7848901.

[4] Samadian, H.; Maleki, H.; Fathollahi, A.; Salehi, M.; Gholizadeh, S.; Derakhshankhah, H.; Allahyari, Z.; Jaymand, M. Naturally Occurring Biological Macromolecules-Based Hydrogels: Potential Biomaterials for Peripheral Nerve Regeneration. *Int. J. Biol. Macromol.* **2020**, *154*, 795–817. DOI: 10.1016/j.ijbiomac.2020.03.155.

[5] Mohammadi, M.; Ramazani SaadatAbadi, A.; Mashayekhan, S.; Sanaei, R. Conductive Multichannel PCL/Gelatin Conduit with Tunable Mechanical and Structural Properties for Peripheral Nerve Regeneration. *Appl. Polym. Sci.* **2020**, *137*, 49219. DOI: 10.1002/app.49219.

[6] Fu, S.; Zhou, L.; Zeng, P.; Fu, S. Antibacterial Chitosan-Gelatin Hydrogel Beads Cross-Linked by Riboflavin under Ultraviolet a Irradiation. *Fibers Polym.* **2022**, *23*, 315–320. DOI: 10.1007/s12221-021-0401-7.

[7] Dulnik, J.; Kołbuk, D.; Denis, P.; Sajkiewicz, P. The Effect of a Solvent on Cellular Response to PCL/Gelatin and PCL/Collagen Electrospun Nanofibres. *Eur. Polym. J.* **2018**, *104*, 147–156. DOI: 10.1016/j.eurpolymj.2018.05.010.

[8] Sadeghi, A.; Moztarzadeh, F.; Aghazadeh Mohandesi, J. Investigating the Effect of Chitosan on Hydrophilicity and Bioactivity of Conductive Electrospun Composite Scaffold for Neural Tissue Engineering. *Int. J. Biol. Macromol.* **2019**, *121*, 625–632. DOI: 10.1016/j.ijbiomac.2018.10.022.

[9] Liu, S.; Sun, L.; Zhang, H.; Hu, Q.; Wang, Y.; Ramalingam, M. High-Resolution Combinatorial 3D Printing of Gelatin-Based Biomimetic Triple-Layered Conduits for Nerve Tissue Engineering. *Int. J. Biol. Macromol.* **2021**, *166*, 1280–1291. DOI: 10.1016/j.ijbiomac.2020.11.010.

[10] Wang, L.; Wu, Y.; Hu, T.; Ma, P. X.; Guo, B. Aligned Conductive Core-Shell Biomimetic Scaffolds Based on Nanofiber Yarns/Hydrogel for Enhanced 3D Neurite Outgrowth Alignment and Elongation. *Acta Biomater.* **2019**, *96*, 175–187. DOI: 10.1016/j.actbio.2019.06.035.

[11] Samadian, H.; Ehterami, A.; Sarrafzadeh, A.; Khastar, H.; Nikbakht, M.; Rezaei, A.; Chegini, L.; Salehi, M. Sophisticated Polycaprolactone/Gelatin Nanofibrous Nerve Guided Conduit Containing Platelet-Rich Plasma and Citicoline for Peripheral Nerve Regeneration: In Vitro and In Vivo Study. *Int. J. Biol. Macromol.* **2020**, *150*, 380–388. DOI: 10.1016/j.ijbiomac.2020.02.102.

[12] Li, D.; Zhao, L.; Cong, M.; Liu, L.; Yan, G.; Li, Z.; Li, B.; Yu, W.; Sun, H.; Yang, B. Injectable Thermosensitive Chitosan/Gelatin-Based Hydrogel Carried Erythropoietin to Effectively Enhance Maxillary Sinus Floor Augmentation in Vivo. *Dent. Mater.* **2020**, *36*, e229–e240. DOI: 10.1016/j.dental.2020.04.016.

[13] Rakhshaei, R.; Namazi, H.; Hamishehkar, H.; Kafil, H.; Salehi, R. In Situ Synthesized Chitosan–Gelatin/ZnO Nanocomposite Scaffold with Drug Delivery Properties: Higher Antibacterial and Lower Cytotoxicity Effects. *J. Appl. Polym. Sci.* **2019**, *136*, 47590. DOI: 10.1002/app.47590.

[14] Rodríguez-Rodríguez, R.; Espinosa-Andrews, H.; Velasquillo-Martínez, C.; García-Carvajal, Z. Y. Composite Hydrogels Based on Gelatin, Chitosan and Polyvinyl Alcohol to Biomedical Applications: A Review. *Int. J. Polym. Mater. Polym. Biomater.* **2020**, *69*, 1–20. DOI: 10.1080/00914037.2019.1581780.

[15] Astaneh, M. E.; Goodarzi, A.; Khanmohammadi, M.; Shokati, A.; Mohandesnezhad, S.; Ataollahi, M. R.; Najafipour, S.; Farahani, M. S.; Ai, J. Chitosan/Gelatin Hydrogel and Endometrial Stem Cells with Subsequent Atorvastatin Injection Impact in Regenerating Spinal Cord Tissue. *J. Drug Delivery Sci. Technol.* **2020**, *58*, 101831. DOI: 10.1016/j.jddst.2020.101831.

[16] Bayat, A.; Ramazani, A.; A, S. Biocompatible Conductive Alginate/Polyaniline-Graphene Neural Conduits Fabricated

Using a Facile Solution Extrusion Technique. *Int. J. Polym. Mater. Polym. Biomater.* **2021**, *70*, 486–495. DOI: 10.1080/00914037.2020.1725764.

[17] Mohseni, M.; A, A. R. S.; H Shirazi, F.; Nemati, N. H. Preparation and Characterization of Self-Electrical Stimuli Conductive Gellan Based Nano Scaffold for Nerve Regeneration Containing Chopped Short Spun Nanofibers of PVDF/MCM41 and Polyaniline/Graphene Nanoparticles: Physical, Mechanical and Morphological Studies. *Int. J. Biol. Macromol.* **2021**, *167*, 881–893. DOI: 10.1016/j.ijbiomac.2020.11.045.

[18] Soleimani, M.; Mashayekhan, S.; Baniasadi, H.; Ramazani, A.; Ansarizadeh, M. Design and Fabrication of Conductive Nanofibrous Scaffolds for Neural Tissue Engineering: Process Modeling via Response Surface Methodology. *J. Biomater. Appl.* **2018**, *33*, 619–629. DOI: 10.1177/0885328218808917.

[19] Azimi, S.; Golabchi, A.; Nekookar, A.; Rabbani, S.; Hassanpour Amiri, M.; Asadi, K.; Abolhasani, M. M. Self-Powered Cardiac Pacemaker by Piezoelectric Polymer Nanogenerator Implant. *Nano Energy* **2021**, *83*, 105781. DOI: 10.1016/j.nanoen.2021.105781.

[20] Azimi, B.; Sorayani Bafqi, M. S.; Fusco, A.; Ricci, C.; Gallone, G.; Bagherzadeh, R.; Donnarumma, G.; Uddin, M. J.; Latifi, M.; Lazzeri, A.; Danti, S. Electrospun ZnO/Poly(Vinylidene Fluoride-Trifluoroethylene) Scaffolds for Lung Tissue Engineering. *Tissue Eng. A* **2020**, *26*, 1312–1331. DOI: 10.1089/ten.TEA.2020.0172.

[21] Chandran, A. M.; Varun, S.; Mural, P. K. S. Flexible Electroactive PVDF/ZnO Nanocomposite with High Output Power and Current Density. *Polym. Eng. Sci.* **2021**, *61*, 1829–1841. DOI: 10.1002/pen.25704.

[22] Chen, C.; Bai, Z.; Cao, Y.; Dong, M.; Jiang, K.; Zhou, Y.; Tao, Y.; Gu, S.; Xu, J.; Yin, X.; Xu, W. Enhanced Piezoelectric Performance of $BiCl_3$/PVDF Nanofibers-Based Nanogenerators. *Compos. Sci. Technol.* **2020**, *192*, 108100. DOI: 10.1016/j.compscitech.2020.108100.

[23] Liu, G.; Tsen, W.-C.; Jang, S.-C.; Hu, F.; Zhong, F.; Zhang, B.; Wang, J.; Liu, H.; Wang, G.; Wen, S.; Gong, C. Composite Membranes from Quaternized Chitosan Reinforced with Surface-Functionalized PVDF Electrospun Nanofibers for Alkaline Direct Methanol Fuel Cells. *J. Membr. Sci.* **2020**, *611*, 118242. DOI: 10.1016/j.memsci.2020.118242.

[24] Liu, X.; Ma, J.; Wu, X.; Lin, L.; Wang, X. Polymeric Nanofibers with Ultrahigh Piezoelectricity via Self-Orientation of Nanocrystals. *ACS Nano* **2017**, *11*, 1901–1910. DOI: 10.1021/acsnano.6b07961.

[25] Yang, J.; Zhang, Y.; Li, Y.; Wang, Z.; Wang, W.; An, Q.; Tong, W. Piezoelectric Nanogenerators Based on Graphene Oxide/PVDF Electrospun Nanofiber with Enhanced Performances by in-Situ Reduction. *Mater. Today Commun.* **2021**, *26*, 101629. DOI: 10.1016/j.mtcomm.2020.101629.

[26] Abzan, N.; Kharaziha, M.; Labbaf, S. Development of Three-Dimensional Piezoelectric Polyvinylidene Fluoride-Graphene Oxide Scaffold by Non-Solvent Induced Phase Separation Method for Nerve Tissue Engineering. *Mater. Des.* **2019**, *167*, 107636. DOI: 10.1016/j.matdes.2019.107636.

[27] Maghfoori, F.; Najmoddin, N.; Pezeshki-Modaress, M. Enhancing Mechanical and Antibacterial Properties of Polycaprolactone Nanocomposite Nanofibers Using Decorated Clay with ZnO Nanorods. *J. Appl. Polym. Sci.* **2022**, *139*, e52684. DOI: 10.1002/app.52684.

[28] Ratanavaraporn, J.; Rangkupan, R.; Jeeratawatchai, H.; Kanokpanont, S.; Damrongsakkul, S. Influences of Physical and Chemical Crosslinking Techniques on Electrospun Type a and B Gelatin Fiber Mats. *Int. J. Biol. Macromol.* **2010**, *47*, 431–438. DOI: 10.1016/j.ijbiomac.2010.06.008.

[29] Kitsara, M.; Blanquer, A.; Murillo, G.; Humblot, V.; De Bragança Vieira, S.; Nogués, C.; Ibáñez, E.; Esteve, J.; Barrios, L. Permanently Hydrophilic, Piezoelectric PVDF Nanofibrous Scaffolds Promoting Unaided Electromechanical Stimulation on Osteoblasts. *Nanoscale* **2019**, *11*, 8906–8917. DOI: 10.1039/C8NR10384D.

[30] Shi, K.; Sun, B.; Huang, X.; Jiang, P. Synergistic Effect of Graphene Nanosheet and BaTiO3 Nanoparticles on Performance Enhancement of Electrospun PVDF Nanofiber Mat for Flexible Piezoelectric Nanogenerators. *Nano Energy* **2018**, *52*, 153–162. DOI: 10.1016/j.nanoen.2018.07.053.

[31] Liu, C.; Shen, J.; Liao, C.; Yeung, K.; Tjong, S. Novel Electrospun Polyvinylidene Fluoride-Graphene Oxide-Silver Nanocomposite Membranes with Protein and Bacterial Antifouling Characteristics. *Express Polym. Lett.* **2018**, *12*, 365–382. DOI: 10.3144/expresspolymlett.2018.31.

[32] Lou, L.; Kendall, R. J.; Smith, E.; Ramkumar, S. S. Functional PVDF/rGO/TiO2 Nanofiber Webs for the Removal of Oil from Water. *Polymer* **2020**, *186*, 122028. DOI: 10.1016/j.polymer.2019.122028.

[33] Bello, A. B.; Kim, D.; Kim, D.; Park, H.; Lee, S.-H. Engineering and Functionalization of Gelatin Biomaterials: From Cell Culture to Medical Applications. *Tissue Eng. B Rev.* **2020**, *26*, 164–180. DOI: 10.1089/ten.teb.2019.0256.

[34] Ojeda-Hernández, D. D.; Canales-Aguirre, A. A.; Matias-Guiu, J.; Gomez-Pinedo, U.; Mateos-Díaz, J. C. Potential of Chitosan and Its Derivatives for Biomedical Applications in the Central Nervous System. *Front. Bioeng. Biotechnol.* **2020**, *8*, 389., DOI: 10.3389/fbioe.2020.00389.

[35] Cristallini, C.; Barbani, N.; Bianchi, S.; Maltinti, S.; Baldassare, A.; Ishak, R.; Onor, M.; Ambrosio, L.; Castelvetro, V.; Cascone, M. G. Assessing two-way interactions between cells and inorganic particles. J. Mater. Sci. Mater. Med. 2020, *31*, 1.

[36] Zare, Y.; Rhee, K. Y.; Hui, D. Influences of Nanoparticles Aggregation/Agglomeration on the Interfacial/Interphase and Tensile Properties of Nanocomposites. *Compos. B Eng.* **2017**, *122*, 41–46. DOI: 10.1016/j.compositesb.2017.04.008.

[37] Jiang, H.; Qian, Y.; Fan, C.; Ouyang, Y. Polymeric Guide Conduits for Peripheral Nerve Tissue Engineering. *Front. Bioeng. Biotechnol.* **2020**, *8*, 582646–582646. DOI: 10.3389/fbioe.2020.582646.

[38] Cheng, Y.; Xu, Y.; Qian, Y.; Chen, X.; Ouyang, Y.; Yuan, W.-E. 3D Structured Self-Powered PVDF/PCL Scaffolds for Peripheral Nerve Regeneration. *Nano Energy* **2020**, *69*, 104411. DOI: 10.1016/j.nanoen.2019.104411.

[39] Parveen, N.; Mahato, N.; Ansari, M. O.; Cho, M. H. Enhanced Electrochemical Behavior and Hydrophobicity of Crystalline Polyaniline@Graphene Nanocomposite Synthesized at Elevated Temperature. *Compos. B Eng.* **2016**, *87*, 281–290. DOI: 10.1016/j.compositesb.2015.10.029.

[40] Song, J.; Sun, B.; Liu, S.; Chen, W.; Zhang, Y.; Wang, C.; Mo, X.; Che, J.; Ouyang, Y.; Yuan, W.; Fan, C. Polymerizing Pyrrole Coated Poly (L-Lactic Acid-co-ε-Caprolactone) (PLCL) Conductive Nanofibrous Conduit Combined with Electric Stimulation for Long-Range Peripheral Nerve Regeneration. *Front. Mol. Neurosci.* **2016**, *9*, 117. DOI: 10.3389/fnmol.2016.00117.

[41] Kim, M.; Fan, J. Piezoelectric Properties of Three Types of PVDF and ZnO Nanofibrous Composites. *Adv. Fiber Mater.* **2021**, *3*, 160–171. DOI: 10.1007/s42765-021-00068-w.

[42] Mahanty, B.; Ghosh, S. K.; Jana, S.; Mallick, Z.; Sarkar, S.; Mandal, D. ZnO Nanoparticle Confined Stress Amplified All-Fiber Piezoelectric Nanogenerator for Self-Powered Healthcare Monitoring. *Sustainable Energy Fuels* **2021**, *5*, 4389–4400. DOI: 10.1039/D1SE00444A.